Experimental and transient/harmonic numerical investigations for the risk assessment of a rotor response after blade off with radial rubbing

Loïc Peletan, Mohamed Torkhani, Ludovic May, Sébastien Baguet, Philipe Voinis, Georges Jacquet Richardet

XVIIIth symposium
Vibrations, Chocs et Bruit* & ASTELAB
*VISHNO (VIbrations, SHocks & NOise)
July 3, 4 and 5, 2012
Centre de recherche EDF
de Clamart

Vibrations, Shocks and Noise

Experimental and transient/harmonic numerical investigations for the risk assessment of a rotor response after blade-off with radial rubbing

Loïc Peletan[a,b]*, Mohamed Torkhani[b], Ludovic May[b], Sébastien Baguet[a], Philipe Voinis[b], Georges Jacquet-Richardet[a]

[a]*LaMCoS INSA Lyon, 18-20 rue des Sciences, Villeurbanne 69100, France*
[b]*LaMSID EDF R&D, 1 Avenue du Général de Gaulle, Clamart 92140, France*

Abstract

In nuclear power plant turbosets, the design-basis accident consists of a blade-off on the low pressure turbine last stage. During the accidental shutdown, a severe rotor-casing contact interaction may occur at critical speeds due to large shaft line displacements originated by a high imbalance excitation. EDF must be able to check that the bearings are capable of withstanding the loads developed during passing through critical speeds in the deceleration phase without catastrophic consequences for the shaft line. The targeted non-linearity is due to frictional rotor-stator contact. The first focus of the paper is EDF's modular EURoPE test rig. This test bench has been designed for experimental investigation of rotor-stator contact during emergency shutdown. The second focus of the paper is on a modeling framework tailored to simulating the overall dynamic behavior of a non linear rotor subjected to imbalance. A 1D-based FE model is used for the entire turbine system. The highly nonlinear equations due to contact conditions are solved through an explicit time-marching procedure combined with the Lagrange multiplier approach dealing with a node-to-line contact strategy. On the other hand, the Harmonic Balance Method (HBM) is also used for fast assessment of the model steady-state response.

Keywords : rotordynamics ; blade-off ; rub-impact ; experimental test bench ; transient simulations ; harmonic balance method

1. Introduction

1.1. Industrial context and problem statement

Turbomachines for aeronautical and terrestrial applications mainly comprise rotating bladed disks, the assembly of which forms a rotor and a non-rotating bladed disks assembly, named the stator. In turbo-machinery, the requirement of higher efficiency has reduced the clearances between shaft (rotating part) and stator (stationary part). The safety of turbomachines involves the control of risk situations such as contact between rotating and stationary parts of the turbine, usually referred to as rubbing (Muszynska [1], Beatty [2]), due to "low unbalance" and accidental situations referred to as "high unbalance". In the first situation, intermittent contacts of low levels will be the location for energy exchange between the rotating part and the fixed part. Various modes can then occur,

* Corresponding author. Tel.: +33-147-653-293.
E-mail address: loic.peletan@insa-lyon.fr.

depending on the speed of rotation of the rotor, the loading and the geometrical and physical parameters of the system. These modes can lead to the loss of contact between the rotor and the stator, but also to unstable phenomena, the consequences of which can prove to be disastrous. The second configuration or high unbalance will lead to severe contact between the rotor and the stator. Rub is usually caused by unbalanced rotor, blade-off, misalignment of the rotor centerline, thermal unbalance, casing excitations. This can occur in the start up procedures of a new machine or of an older one after a shutdown and must be taken into consideration in the design of the machine. In this study, the shaft-diaphragm interaction only is considered: indeed, in real turbosets, the blades-to-diaphragm contact is negligible in comparison to the shaft-stator interaction.

To do this, rub experiments were performed on the "EURoPE" modular test rig of EDF R&D. The test rig has been designed in order to be as much as possible representative of industrial machines, mainly steam turbines of power plants. This rig has been employed for several researches in the field of rotor dynamics (see Stoisser et al. [3]). In the first rig configuration of the shaftline without inertia flywheels (see [4]), the shutdown transient and rubbing durations were very short (respectively less than 50 and 10 seconds). These durations did not enable us to investigate all the physical phenomena. Thus, it was decided to go on with the rubbing experiments in order to ensure through a more representative configuration (EURoPE shaftline with inertia flywheel) whether the Rotor-Stator contact generates or not complex and uncontrolled phenomena. The current configuration allows for longer contact and shutdown durations. The phenomenological analyses will be undertaken on the basis of the test results in this configuration. Indeed, the presence of the inertial flywheel can a priori imply the following effects:

- amplification of the gyroscopic effects;
- variation of the shaft deformation across the rotating speed at which the contact occurs;
- decrease of the critical speed;
- possibilities of persistent Rotor-Stator contact (leading to full annular rubbing) and backward whirling motion.

1.2. Article focus

In order to verify the foregoing physical explanations of rubbing phenomena, theoretical predictions and experimental observations were performed. A test rig has been designed to allow for rubs to a rotating shaft during start-up and shutdown operating conditions. A description of the experimental rig and the procedures used to investigate the dynamical responses of the system are presented. This small test rig cannot be fully representative of the behavior of a big sized real machine. However scaling effects have been considered. It is then expected that some valuable vibration features of the rub-impact rotor system can be observed and the research can provide some useful information for the fault diagnostics of rotating machinery.

The experiments were performed under different conditions to observe the nonlinear vibrations. For instance, a gradual unbalancing of the rotating shaft is used to generate rubs of different intensities. Some quantities have been measured: shaft vibrations in the section where contact occurs, forces transmitted to the supporting structure, duration of contact and angular decelerations.

Investigations of the motion of the rotor with rubbing experimental methods in the case of 'large' are presented in this paper. The general framework for numerical investigations is also presented.

2. Description of the experimental setup

2.1. Description of the EURoPE test rig

The bench is a two-fluid bearing horizontal rotor system (see Figure 1). The flexible shaft is composed of three rotors, with a central modulus that can be modified or replaced in order to study different contact samples. The overall shaft length is 3150mm with a nominal diameter of 210mm. The shaft is connected to an electrical motor, driven by inverter, by means of a flexible coupling. The total shaft mass is approximately 450kg and the main inertia disk has a mass of about 250kg. The first and second bending mode frequencies of the rotor system are respectively

close 17.3Hz and 19.4Hz at nominal rotating speed (1500rpm). The first torsion mode is equal to 84Hz. The motor drives the shaft from 0rpm up to a maximum design rotating speed of 3000rpm, but tests are generally carried out at lower speeds, because the aim is to analyze the behavior in the neighborhood of the first flexural critical speed under safe conditions.

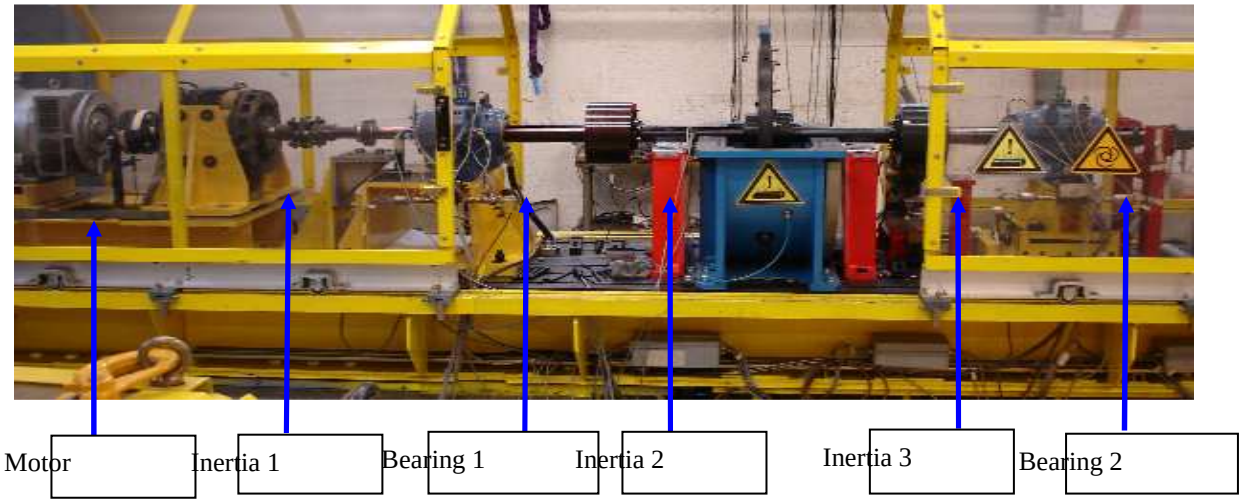

Figure 1 EDF R&D EURoPE test rig

The shaft is supported by two equal lemon shaped oil-film bearings and by two bearing housings, connected to an oil circulation system to lubricate the bearings. The supporting structure can be considered as rigid in the considered speed range. The bearings are equipped with two proximity probes in the horizontal and vertical directions for the measurements of relative shaft-journal vibrations. The casings are equipped with two accelerometers for measuring its vibrations in vertical and horizontal directions. Probes, located near each bearing and near the contact position, measure the shaft vibrations in vertical and horizontal directions.

In order to better simulate the real process of the rub, we have designed a special structure of stator that can make it possible to perform a safe and reliable contact experiment, as shown in Fig. 2.

Figure 2 View of the stator and the contact zone

It is easy for the stator to be mounted, disassembled or interchanged. Not only can the concentricity of the stator and the rotor be adjusted, but also the clearance is adjustable by changing the different inner stators. In fact, different materials (respectively Steel, Teflon and Brass) can be used for the inner part of the stator in order to meet different experimental conditions. However, this leads to some difficulties to have a valid reference case. In fact, by considering two rundowns of the rotor with and without mounted stator, small differences in the unbalance sensitivity of the shaftline might be introduced when the stator is assembled to or disassembled from the whole structure. The stator structure is clamped to a massive concrete block by means of four bolts.

Force sensors are installed between the contact interface and the casing in order to measure the forces generated by the contact interaction.

Tests were carried out to check the effectiveness of the sensor system to measure the contact forces.

2.2. Validation of the unbalance procedure

Our primary objective is to study the rubbing phenomena only during the accidental shutdown. Then, a dedicated device was designed to guarantee no-rubbing conditions during the speed-up of the shaftline ("well-balanced" shaftline). The idea consists in the excitation of the shaft by unbalance force only during rundown. The principle relies on installing on the stator a case in which one places a known mass made up of water ice block. The mass of ice block corresponds to the unbalance which one wishes to impose on the machine during the rundown. The case (called "IceCase") is in correspondence of the second inertia disc with a mass eccentricity of 105mm and an angular position of 30° compared to the Top-Tour (phase reference). To balance the machine during the run-up, one has to install a compensation mass (called "CMass") in phase opposition with the "IceCase" (i.e. with a 210° angular position). These positions were found experimentally in order to make it possible to maximize the vibration amplitude of the shaftline in the contact zone. Actually, one must manage to have in-phase vibrations due to the unbalance and to rotor bow over the first critical speed. Since this varying unbalance must not exceed a maximum authorized value (security issue), a fixed unbalance of 8.3g is placed in correspondence of the first inertia disc with a mass eccentricity of 250mm and an angular position of 345°. This second unbalance aims at "helping" the balancing procedure. Figure 3 represents the prototype.

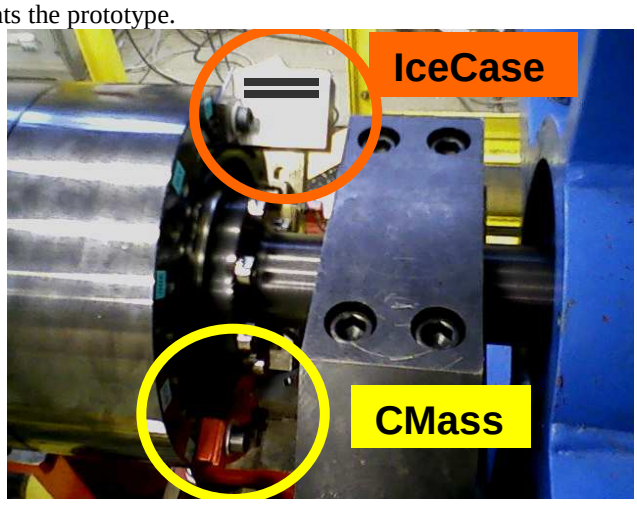

Figure 3 Ice block case and compensation mass installed on the second inertia disc of the test rig

Thus, the "well-balanced" shaft is driven by the motor to run up until the rotating speed of 1525rpm. This guarantees that the rubbing will not occur until the ice has completely melt (larger unbalance amount generates larger vibration amplitudes). During heavy contact tests, the stabilization speed was raised to 1640rpm. Once this

rated speed reached, one has to wait for complete ice melting, i.e. until full stabilization of the vibration levels. The shaftline is then subjected to an unbalance corresponding to the "CMass" mass. One cuts then the engine supply off in order to allow for shaftline free rundown. The vibration of the shaftline is then directly correlated with the compensation mass.

Tests with unbalances (applied to the shaft balancing plane) have been run in order to check the sensitivity of the bearing response to unbalancing forces and to identify all resonances of the system. This model and its results were used to plan the experiments and to aid in the balancing procedures.

Results show that the unbalance device is fully operational and that the force sensors assembly allows for measuring the instantaneous forces. The test rig is then suitable for rubbing tests to be performed.

The following characteristics have been measured on the bench: rotor-stator radial clearance equal to 400µm, radial rotor eccentricity equal to 105µm and radial rotor bow equal to 75µm. When radial deflection exceeds the remaining clearance between the external surface of the whirling shaft and the internal surface of the stationary part, then contact occurs.

2.3. Analysis of experimental results - case of heavy contact

After setting up the rig, some first experimental results have been obtained. In order to operate in safe conditions towards the contact severity, we adopted a gradual modification of inner stator material (Teflon, Brass then Steel) and a gradual increase in the unbalance amount. Moreover, since rubbing is a kind of nonlinear phenomena, the experimental results cannot be the same at every time. In this respect, several experiments for a set-up need to confirm a peculiar physical phenomenon. Through these several experiments the noise and the signal can be manifested. In our case, tests were carried out several times in order to ensure a "repeatability" of the experimental results. Doing this, we can avoid signals noise while also controlling all the procedures of the set-up.

Results obtained during the rundown will be shown in terms of shaft orbits, contact duration, contact force and rotational speed variation. Values recorded by force sensors represent only roughly the contact forces because the measured forces are affected by the inertia forces of the ring support. Orbits in presence of rub are obtained also in bearings but are omitted here for clarity.

The unbalance mass amount used to simulate heavy contact is 77.15g, which corresponds to a total applied unbalance of 0.0017Kg.m on disc 1 plus 0.0081Kg.m on disc 2. The corresponding shaft vibrations amplitudes are plotted in Fig. 4. Two main events are observed from the vibration measures. They correspond to:

- appearance of shocks in the signal measured by the force sensors. The contact initiation is recorded by the sensor beginning from 1173rpm (right cursor in Fig. 4).
- extinction of the shock from the force sensor after 964rpm (left cursor in Fig. 4).

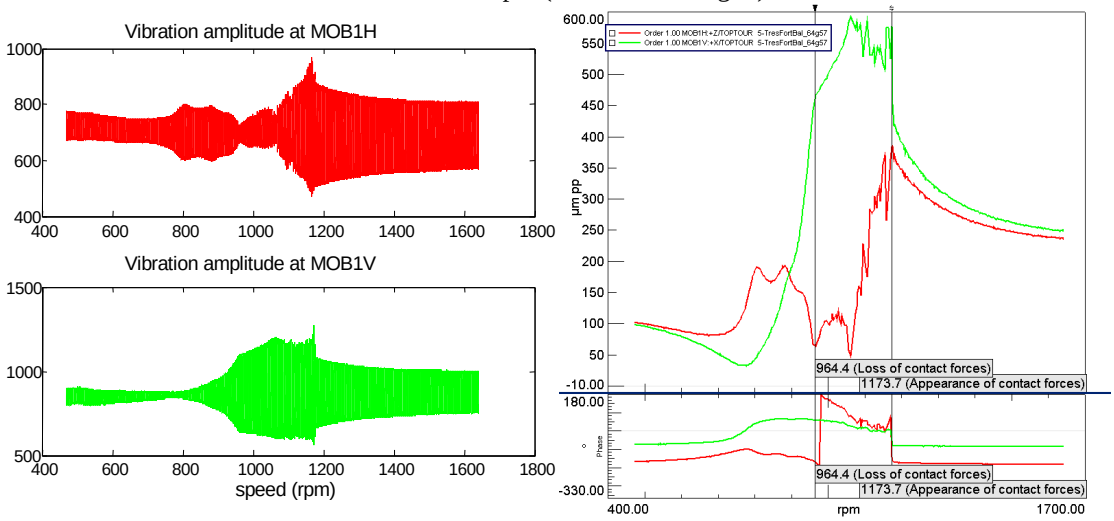

Figure 4 rotor vibrations measured in the plane MOB1 for an unbalance of 77.15g

Figure 5 illustrates, in a few images, the rotor orbit during the contact phase.

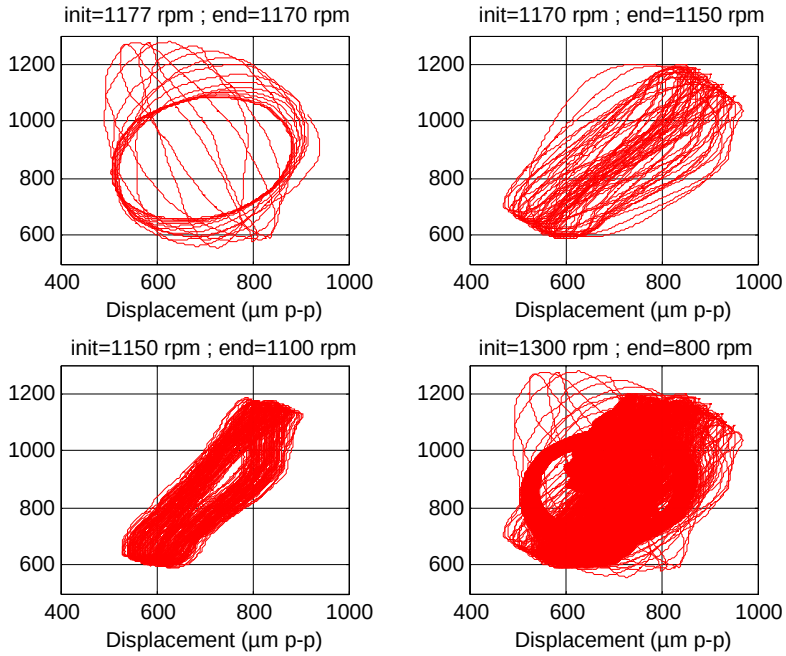

Figure 5 measured rotor orbit at sensor MOB1 for a 77.15g unbalance

Similarly to the previous case, the triggering of the contact is located in the upper part of the inner stator before the shaft crosses its critical speed. Image 2 shows severe intermittent rub conditions are experienced, contacts with rebounds occur (three contact points per revolution).

Under severe rub conditions, worth mentioning is the fact that the orbit is significantly enlarged and that it presents a more irregular shape during rub. In fact, one observes an almost triangular strongly distorted trajectory at the contact location during a few rotor revolutions. This behavior is due to sub-harmonic components and rub effects which contribute significantly, besides the 1x component, to compose the orbit. Some revolutions later (Image 4), there is no more than 2 contacts per revolution.

In this case, the rotor/stator coupling induces an augmentation of the shaft critical speed of about 70rpm. The contact forces reach values up to 1500N during the shut down.

The time interval during which contacts happen is more than a quarter of the period of revolution.

As previously specified the rotational speed has also been measured with a Top-Tour, which by numerical time derivation gives the angular accelerations. The angular velocity and deceleration graphs are shown in Figure 6. The measured rotation speed curve depicts clearly a visible modification with the naked eye at the shock time.

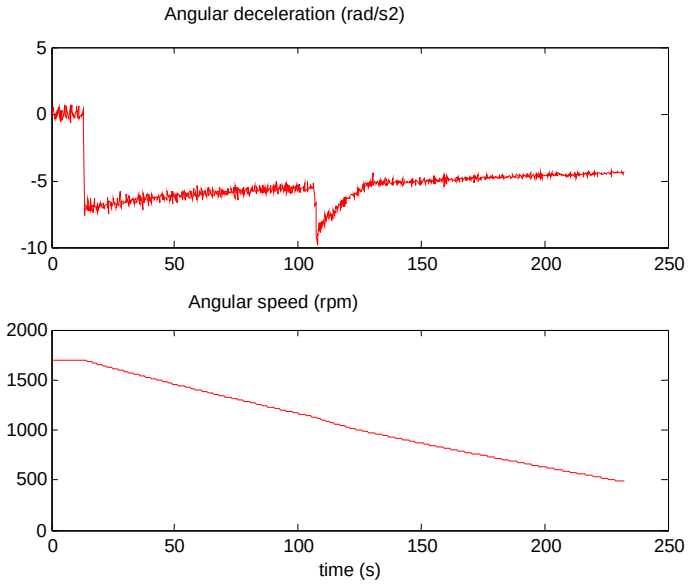

Figure 6 measured angular velocity (left) and deceleration (right)

The angular deceleration graph shows:

- a first phase of null acceleration corresponding to the shaft whirling at the stabilized speed,
- a second phase of strictly negative acceleration corresponding to the natural deceleration of the whirling shaft in absence of rubbing,
- a third phase of slope break in the deceleration curve corresponding to the shock.

Besides the natural deceleration, the friction torque acting on the rotor has the effect to decelerate it.

3. Modeling and simulation results

3.1. The EURoPE test rig model

A 1D finite element numerical model of the test rig is developed in order to run numerical simulations. It is displayed in Fig. 7.

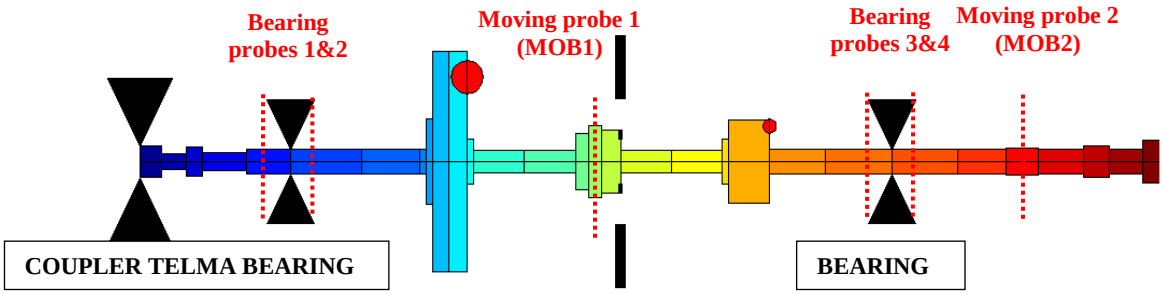

Figure 7 model of the EURoPE test rig

The shaftline rests on 2 bearings, the characteristics of which are modeled by linear stiffness and damping coefficients. A simplified model of the foundation is taken into account at the bearing positions: mass, stiffness and damping coefficients.

The experimental identification of rotor modes is carried out at different rotating speeds in the vicinity of the first critical speed. The resonance rotating speeds are respectively equal to 1053rpm (mode 1) and 1148rpm (mode 2).

To validate the 1D numerical model of the test rig mass and stiffness model parameters are first updated considering the shaft in free–free conditions. The stiffness and damping coefficients of the bearings and the flexible coupling are determined and then adjusted in order to obtain the experimental vibration level related to the well-balanced shaftline. Eigen frequencies and reduced damping values obtained using the updated FE model are successfully compared to the corresponding experimental values. The values of frequency show very good accordance between numerical and experimental results. Residual damping is also well reproduced by the numerical model, whilst a discrepancy of the first mode residual damping is observed for low and high rotating speeds (i.e. away from the critical speed). The accuracy of the shaftline model is thus verified at least in the vicinity of the first critical speed.

In order to predict the behavior of the bench, two different numerical methods will be used and their results will be shown during the presentation. The two methods are described hereafter. They both solve the equation of motion resulting from the space FEM discretisation of the rotor (see Roques et al. [5] for more details):

$$\mathbf{M}\ddot{\mathbf{q}}(t) + \mathbf{C}\dot{\mathbf{q}}(t) + \mathbf{K}\mathbf{q}(t) + \mathbf{f}\big(\mathbf{q}(t)\big) - \mathbf{p}(t) = \mathbf{0} \tag{1}$$

where $\mathbf{q}$ represents the displacement vector for all of the n degrees of freedom (DOFs); $\mathbf{K}$, $\mathbf{C}$ and $\mathbf{M}$ are the generalized $n \times n$ stiffness, damping and mass matrices; $\mathbf{f}$ is the nonlinear force vector and $\mathbf{p}$ is the external excitation force vector.

As a general statement $\mathbf{C} = \dot{\varphi}\mathbf{G} + \mathbf{A}_{\text{bearings}}$, where $\mathbf{G}$ is the gyroscopic matrix, $\mathbf{A}_{\text{bearings}}$ is the bearings damping matrix and φ is the angular position of the shaftline. $\mathbf{K} = \mathbf{K}_{\text{shaft}} + \mathbf{K}_{\text{bearing}} + \ddot{\varphi}\mathbf{K}_{\text{stiff}}$ where $\mathbf{K}_{\text{shaft}}$ is the shaftline stiffness matrix, $\mathbf{K}_{\text{bearing}}$ is the bearings stiffness matrix and $\mathbf{K}_{\text{stiff}}$ is the stiffness matrix due to angular velocity variations.

$$\mathbf{p}(t) = \sum_{i=1}^{N_{\text{unbalance}}} m_i r_i [(\ddot{\varphi}\sin\varphi + \dot{\varphi}^2\cos\varphi)\mathbf{p}_1 + (-\ddot{\varphi}\cos\varphi + \dot{\varphi}^2\sin\varphi)\mathbf{p}_2]$$

where m_i is the unbalance mass and r_i is the unbalance excentricity. $\mathbf{p}_1$and $\mathbf{p}_2$ are unit vectors.

3.2. Harmonic Balance Method for fast assessment of the system behavior

The Harmonic Balance Method (HBM) is a well known technique, used to compute periodic solutions for dynamic systems. This method consists in solving the equations of movement in the frequency domain, rather than in the time domain. As the movement is supposed periodic, the transient effects are not taken into account. Thus, the angular velocity is considered constant ($\ddot{\varphi} = 0$) in the above equations.

When the external excitations are periodic, it is valid to assume that a steady state solution for Eq. (1) exists, and that this solution is also periodic. The displacements can thus be written as a truncated Fourier series:

$$\mathbf{q}(t) = \mathbf{Q}_0 + \sum_{j=1}^{N} (\mathbf{Q}_{2j-1}\cos(m_j\omega t) + \mathbf{Q}_{2j}\sin(m_j\omega t)) \tag{2}$$

where $\mathbf{Q}_i, i \in [0 \dots 2N]$, are the Fourier coefficients of $\mathbf{q}$; ω is the fundamental pulsation of the external excitation, and $m_j,\ j \in [0 \dots N]$ are positive integers.

Similarly, $\mathbf{f}(\mathbf{q})$ and $\mathbf{p}(t)$ can be rewritten using the same form:

$$\mathbf{p}(t) = \mathbf{P}_0 + \sum_{j=1}^{N} (\mathbf{P}_{2j-1} \cos(m_j \omega t) + \mathbf{P}_{2j} \sin(m_j \omega t)) \tag{3}$$

$$\mathbf{f}(t) = \mathbf{F}_0 + \sum_{j=1}^{N} (\mathbf{F}_{2j-1} \cos(m_j \omega t) + \mathbf{F}_{2j} \sin(m_j \omega t)) \tag{4}$$

As described in [6] Eqs. (2) (3) and (4) can be substituted into Eq. (1), following which a Galerkin procedure is applied to transform the nonlinear differential Eq. (1), of dimension n, into an algebraic nonlinear system of equations, of dimension $n_{\mathrm{HBM}} = n(2N+1)$:

$$\mathbf{R}(\mathbf{Q}, \omega) = \mathbf{Z}(\omega)\mathbf{Q} + \mathbf{F}(\mathbf{Q}) - \mathbf{P} = \mathbf{0} \tag{5}$$

where:

$$\mathbf{Z} = \mathrm{diag}\left(\mathbf{K}, \begin{bmatrix} \mathbf{K} - m_1^2\omega^2\mathbf{M} & m_1\omega\mathbf{C} \\ -m_1\omega\mathbf{C} & \mathbf{K} - m_1^2\omega^2\mathbf{M} \end{bmatrix}, \cdots, \begin{bmatrix} \mathbf{K} - m_N^2\omega^2\mathbf{M} & m_N\omega\mathbf{C} \\ -m_N\omega\mathbf{C} & \mathbf{K} - m_N^2\omega^2\mathbf{M} \end{bmatrix}\right)$$

$\mathbf{Q} = [\mathbf{Q}_0^T, \mathbf{Q}_1^T, \cdots, \mathbf{Q}_{2N}^T]^T$, $\mathbf{F} = [\mathbf{F}_0^T, \mathbf{F}_1^T, \cdots, \mathbf{F}_{2N}^T]^T$ and $\mathbf{P} = [\mathbf{P}_0^T, \mathbf{P}_1^T, \cdots, \mathbf{P}_{2N}^T]^T$ are the vectors of the Fourier coefficients for displacements, nonlinear forces and external excitations, respectively.

Equation (5) needs to be solved for $\mathbf{Q}$. As this equation is still nonlinear, an appropriate nonlinear solver must be used to derive a correct solution. In the present situation, a Newton-Raphson solver is used. The Newton-Raphson solves Eq. (5) in an iterative manner :

$$\mathbf{Q}^{(k+1)} = \mathbf{Q}^{(k)} + \left(\frac{\partial \mathbf{R}(\mathbf{Q}^{(k)})}{\partial \mathbf{Q}}\right)^{-1} \mathbf{R}(\mathbf{Q}^{(k)}, \omega)$$

It has been demonstrated that the combined use of HBM and a Newton-Raphson solver is equivalent to the Incremental Harmonic Balance Method (IHBM) [7].

An Alternating Frequency Time (AFT) algorithm [8] was used for the computation of $\mathbf{F}(\mathbf{Q})$, and as the relationship between the displacements and the nonlinear forces is known only in the time domain (i.e. is a priori unknown in the frequency domain), direct and inverse Fourier transforms must be used to determine $\mathbf{F}(\mathbf{Q})$. The displacements ($\mathbf{Q}$) in the frequency domain are transferred to the time domain using an inverse Fourier transform. Once the time domain displacements ($\mathbf{q}$) are known, the (time-domain) nonlinear forces ($\mathbf{f}(\mathbf{q})$) can be calculated. A direct Fourier transformation is then performed, to obtain the nonlinear forces in the frequency domain ($\mathbf{F}$). The next Newton-Raphson iteration can then be carried out. In practice, fast Fourier transform algorithms (FFT) are used due to their combined speed, accuracy and robustness. This procedure can be summarized as follows:

$$\mathbf{Q}(\omega) \xrightarrow{\mathrm{fft}^{-1}} \mathbf{q}(t) \rightarrow \mathbf{f}(t) \xrightarrow{\mathrm{fft}} \mathbf{F}(\omega)$$

Similarly, the Jacobian term, $\frac{\partial \mathbf{R}(\mathbf{Q}^{(k)})}{\partial \mathbf{Q}}$, is calculated via analytical derivation rather than through the use of finite differences, in order to ensure better accuracy and faster convergence. A pseudo-arc length continuation method [9] is used for the parametric study.$\mathbf{R}(\mathbf{Q}, \omega) = \mathbf{Z}(\omega)\mathbf{Q} + \mathbf{F}(\mathbf{Q}) - \mathbf{P} = \mathbf{0}$

3.3. Numerical time integration strategy

The second method solves Eq. (1) using a time integration scheme. The transient effects are taken into account. The angular deceleration which is originated by contact between the shaftline and the stator (considered as an unknown) is taken into account. So an additional equation computes the instantaneous rotating speed depending on the contact forces.

The highly nonlinear equations due to contact conditions are solved through an explicit prediction–correction time-marching procedure combined with the Lagrange multiplier approach dealing with a node-to-line contact strategy. In our study, a Finite Central Differences scheme combined with Lagrange multipliers (prediction-correction algorithm) properly satisfies the contact detection and ensures the compatibility of the speed and the acceleration. The chosen time step Δt is equal to10^{-6} s, so that convergence of the quantities of interest with respect to the time step is achieved.

4. Conclusion

The emphasis of this paper was twofold: to emphasize experimental physical phenomena and to present a modeling framework for two kinds of numerical simulations.

An experimental set-up was constructed to investigate the partial rub of a rotor due to contact with a non-rotating obstacle. The dedicated experimental bench as proposed is believed to be capable to simulate the rubbing phenomena which may occur in real rotating machinery. For highly-unbalanced rotating machines (generating “heavy” contact), some new characteristics are pointed out, primarily with regard to the orbit shape of the rotor. By examining more deeply the various phases of the measured orbit, one can say that this discrepancy could be caused by a very marked local deformation of the casing. This kind of casing “resonance” could be induced by the great flexibility of the casing or the bad attachment of the stator to its supporting structure. Recent investigations in the experimental set-up show that the stator is rather badly attached to its supporting structure than excessively flexible. The use of an “advanced” fully flexible diaphragm which incorporates the main features of the true structure (particularly realistic attachment conditions) seems to be mandatory for an accurate prediction of the bearing loads.

The suggested numerical approaches rely on finite element modeling for both the shaft and the stator. Firstly, the Harmonic Balance Method (HBM) has been presented which allows for fast assessment of the global nonlinear behavior of the system. This method solves the equation of motion in the frequency domain. The movement is thus supposed as periodic. On the other hand a time integration approach has also been presented which allows the transient effects to be taken into account. The combination of these two methods is believed to allow restricting the use of long transient simulations to a minimum.

Further investigations are required in the next future in order to analyze deeply different conditions other than stable light to heavy intermittent rubs, such as continuous full annular rub and even instable backward whirling motions. Moreover, an issue of a bad attachment of the stator to its structure will also be addressed. Simulations of more complex transient rubbing will then be performed and corresponding results will be confronted to experimental ones and reported in a forthcoming paper.

Acknowledgements

The authors express their gratitude to the researchers and the engineers of EDF R&D AMA Department. This work has been also partially supported by the French National Agency (ANR) in the frame of its Technological Research COSINUS program. (IRINA, project *ANR 09 COSI 008 01 IRINA*).

References

[1] A. Muszynska, Rotor to stationary element rub related vibration phenomena in rotating machinery – literature survey, Shock and Vibration Digest (1989) 3–11.
[2] R.F. Beatty, Differentiating rotor response due to radial rubbing, Journal of Vibration, Acoustics, Stress, and Reliability in Design 107 (1985) 151–160.
[3] C. M. Stoisser, S. Audebert, A comprehensive theoretical, numerical and experimental approach for crack detection in power plant rotating machinery. Mechanical Systems and Signal Processing 22 (2008) 818–844.
[4] M. Torkhani, L. May, P. Voinis, Light medium and heavy partial rubs during speed transients of rotating machines: Numerical simulation and experimental observation, Mechanical Systems and Signal Processing 29 (2012), 48—66.
[5] S. Roques, C. Stoisser, P. Cartraud, C. Pierre, B. Peseux, Modelling of rotor speed transient with rotor to stator contact, IFToMM 7th Int. Conf. on Rotor Dynamics Vienna Austria September 25-28 (2006).
[6] E. P. Petrov, D. J. Ewins, Analytical formulation of friction interface elements for analysis of nonlinear multi-harmonic vibrations of bladed disks, Journal of Turbomachinery 125 (2003) 364--371.
[7] S. L. Lau, Y. K. Cheung, S. Y. Wu, A variable parameter incrementation method for dynamic instability of linear and nonlinear elastic systems, Journal of Applied Mechanics 49 (1982) 849--853.
[8] T. M. Cameron, J. H. Griffin, An alternating frequency/time domain method for calculating the steady-state response of nonlinear dynamic systems, Journal of Applied Mechanics 56 (1989) 149--154.
[9] P. Sundararajan, S. T. Noah, An algorithm for response and stability of large order non-linear systems - application to rotor systems, Journal of Sound and Vibration 214 (1998) 695—723.